amplitudes of the twin beams, $\langle\Delta(\hat{X}_s-\hat{X}_i)^2\rangle$ and $\langle\Delta(\hat{Y}_s+\hat{Y}_i)^2\rangle$:

$$\langle\Delta(\hat{X}_{ks}-\hat{X}_{ki})^2\rangle=\langle\Delta(\hat{Y}_{ks}+\hat{Y}_{ki})^2\rangle=\frac{1}{[\cosh(r_kG)+\sinh(r_kG)]^2}. \tag{28}$$

Substituting Eq. (28) into the inseparability coefficient $I_k=\langle\Delta(\hat{X}_{ks}-\hat{X}_{ki})^2\rangle+\langle\Delta(\hat{Y}_{ks}+\hat{Y}_{ki})^2\rangle<2$ [27], we have

$$I_k=\frac{2}{[\cosh(r_kG)+\sinh(r_kG)]^2}<2, \tag{29}$$

which indicates that for signal and idler beams, described by the pair of mode functions $\phi_k(\omega_s)$ and $\psi_k(\omega_i)$, the Duan's inseparability criterion of entanglement is satisfied [27]. Equation (29) clearly shows that I_k always decreases with the gain coefficient G and trends to zero as G approaches to infinity. However, for a fixed coefficient G, the value of I_k increases with the mode index k because the mode amplitude r_k decreases with the increase of k. It is worth noting that if the JSF of the FOPA is spectrally factorable, i.e., $F(\omega_s,\omega_i)=\phi(\omega_s)\psi(\omega_i)$, we have $r_k=\delta_{k,1}$. In this case, only the fundamental mode exists, and I_k in Eq. (29) is the same as that in Ref. [21], describing a CW pumped FOPA operated as a single mode parametric amplifier.

4. Detection of quadrature entanglement

Having demonstrated that the entangled signal and idler twin beams can be decomposed into many pairs of SVD modes, in this section, we will formulate a homodyne detection (HD) process and analyze how to improve the measured degree of entanglement. For simplicity, we assume the polarization states of the individual signal (idler) field and its local oscillator of the HDs (HDi), LOs (LOi), are identical. So the optical fields can be represented as scalars.

The principle of measuring the quadrature components of signal and idler field by using homodyne detectors, HDs and HDi, is shown in the area framed by the dash-dotted line in Fig. 1. The HDs/HDi is comprised of a 50/50 beam splitter (BS) and two photodiodes (PD). Because the signal and idler twin beams are pulsed fields, we take the local oscillators, LOs and LOi, as transform-limited pulses in the form of

$$E_{Ls(Li)}(t)=|\alpha_{Ls(Li)}|e^{i\theta_{Ls(i)}}\int A_{Ls(Li)}(\omega)e^{-i\omega t}d\omega+c.c., \tag{30}$$

where the amplitude of LOs (LOi) is much higher than that of the signal (idler) field, i.e., $|\alpha_{Ls(Li)}|>>1$, $\theta_{Ls(i)}$ represents the phase of LOs (LOi), and $A_{Ls(Li)}(\omega)$ is the spectrum of LOs (LOi) satisfying the normalization condition $\int|A_{Ls(Li)}(\omega)|^2d\omega=1$. The overall efficiency of the HDs (HDi), including the transmission efficiency of the optical paths and the quantum efficiency of the photodiodes, is denoted by $\eta_{s(i)}$, and can be modeled by a beam splitter with transmission efficiency $\eta_{s(i)}$. In this case, the detected field operators of individual signal and idler beams, $\hat{c}_s(\omega_s)$ and $\hat{c}_i(\omega_i)$, are written as

$$\hat{c}_s(\omega_s)=\sqrt{\eta_s}\hat{b}_s(\omega_s)+i\sqrt{1-\eta_s}\hat{v}_s(\omega_s) \tag{31}$$

$$\hat{c}_i(\omega_i)=\sqrt{\eta_i}\hat{b}_i(\omega_i)+i\sqrt{1-\eta_i}\hat{v}_i(\omega_i), \tag{32}$$

where $\hat{v}_s(\omega_s)$ and $\hat{v}_i(\omega_i)$ are vacuum operators introduced by the optical losses.

When the response times of the HDs and HDi are much longer than the pulse durations of signal, idler, LOs, and LOi fields, the result of the homodyne detection can be treated as a time integral of the optical fields. The photocurrent out of HDs and HDi are expressed as [28]:

$$\hat{i}_{s(i)}=q\int_{-\infty}^{\infty}[E_{Ls(Li)}\hat{E'}^{(-)}_{s(i)}+h.c.]dt, \tag{33}$$

#250441 Received 18 Sep 2015; accepted 27 Oct 2015; published 2 Nov 2015

where

$$\hat{E}'^{(-)}_{s(i)} = \frac{1}{\sqrt{2\pi}} \int \hat{c}_{s(i)}(\omega) e^{-i\omega t} d\omega. \tag{34}$$

is the field operator of the detected signal (idler) beam, and the coefficient g is proportional to the electrical gain of detectors.

Since the decomposed modes functions, $\phi_k(\omega_s)$ and $\psi_k(\omega_i)$, form a complete and orthogonal set in the frequency domain of signal and idler beams, the spectra of LOs and LOi (see Eq. (30)) can be expanded into the Fourier series:

$$A_{Ls}(\omega_s) = \sum_k \xi_{ks} \phi_k(\omega_s) \tag{35a}$$

$$A_{Li}(\omega_i) = \sum_k \xi_{ki} \psi_k(\omega_i), \tag{35b}$$

with

$$\xi_{ks} = |\xi_{ks}| e^{-i\theta_{ks}} = \int_S A_{Ls}(\omega_s) \phi_k^*(\omega_s) d\omega_s \tag{36a}$$

$$\xi_{ki} = |\xi_{ki}| e^{-i\theta_{ki}} = \int_I A_{Li}(\omega_i) \psi_k^*(\omega_i) d\omega_i, \tag{36b}$$

where the complex coefficient ξ_{ks} (ξ_{ki}) characterizes the mode matching, $|\xi_{ks}|^2$ ($|\xi_{ki}|^2$) can be viewed as the mode-matching efficiency, and θ_{ks} (θ_{ki}) can be viewed as the relative phase between the kth order signal (idler) mode $\phi_k(\omega_s)$ ($\psi_k(\omega_i)$) and LOs (LOi). Using Eqs. (30) and (35), the photocurrents in Eq. (33) can be rewritten as

$$\hat{i}_s = q|\alpha_{Ls}| \sum_k |\xi_{ks}| [\sqrt{\eta_s} \hat{X}_{ks}(\theta_s) + \sqrt{1-\eta_s} \hat{X}_v] \tag{37a}$$

$$\hat{i}_i = q|\alpha_{Li}| \sum_k |\xi_{ki}| [\sqrt{\eta_i} \hat{X}_{ki}(\theta_i) + \sqrt{1-\eta_i} \hat{X}_v], \tag{37b}$$

where

$$\hat{X}_{ks(ki)}(\theta_{s(i)}) = \frac{1}{\sqrt{2}} (e^{-i\theta_{s(i)}} \hat{B}_{ks(ki)} + e^{i\theta_{s(i)}} \hat{B}^\dagger_{ks(ki)}). \tag{38}$$

with $\theta_{s(i)} = \theta_{Ls(i)} + \theta_{ks(i)}$ denoting the phase angle of the quadrature component of kth order signal (idler) mode, and $\hat{X}_v$ is the quadrature operator of the vacuum field. For the case of $\theta_s = \theta_i = 0$ and $\theta_s = \theta_i = \pi/2$, respectively, $\hat{X}_{ks(ki)}(\theta_{s(i)})$ corresponds to the quadrature amplitude and quadrature phase defined in Eq. (25). Note that in order to clearly demonstrate the mode mismatching effect on measured degree of entanglement, in the analysis hereinafter, we will assume the transmission efficiency of twin beams and detection efficiency of detectors are ideal, i.e., $\eta_s = \eta_i = 1$.

4.1. The spectrum of the LO is matched to a specified SVD mode

When the spectra of LOs and LOi are the same as a pair of decomposed temporal mode, say the kth order modes, Eq. (35) is simplified as

$$A_{Ls}(\omega_s) = \phi_k(\omega_s) \tag{39a}$$

$$A_{Li}(\omega_i) = \psi_k(\omega_i), \tag{39b}$$

and the general expression of the complex coefficients in Eq. (36) becomes $\xi_{sk} = \xi_{ik} = 1$ and $\xi_{sl} = \xi_{il} = 0$ ($l \neq k$) because of the orthogonality. In this case, only the signal and idler fields

#250441 Received 18 Sep 2015; accepted 27 Oct 2015; published 2 Nov 2015

described by the mode functions $\phi_k(\omega_s)$ and $\psi_k(\omega_i)$, respectively, will contribute to the photocurrents in Eq. (37). The evolution of the detected signal and idler fields is described by Eqs. (17) and (18) with an effective gain of $G_{eff} = r_k G$, and the measured inseparability I_k is given by Eq. (29), which goes to zero as G becomes infinitely large.

Among the decomposed SVD modes, the fundamental mode ($k = 1$) has the largest mode amplitude r_1, so its effective parametric gain $G_{eff} = r_1 G$ is the highest. Hence, we can obtain the highest degree of entanglement when the spectra of LOs and LOi are shaped to satisfy the conditions $A_{Ls}(\omega_s) = \phi_1(\omega_s)$ and $A_{Li}(\omega_i) = \psi_1(\omega_i)$. In particular, when the JSF of the FOPA is factorable, i.e., $F(\omega_s, \omega_i) = \phi(\omega_s)\psi(\omega_i)$, and the spectra of LOs and LOi satisfy the conditions $A_{Ls}(\omega_s) = \phi(\omega_s)$ and $A_{Li}(\omega_i) = \psi(\omega_i)$, we will obtain the maximum degree of entanglement for a given gain parameter G because $r_1 = 1$ and $r_k = 0$ ($k \neq 1$), which means all the energy of twin beams is concentrated in the fundamental mode. However, it is worth pointing out that the factorable JSF is not a necessary condition for obtaining the entanglement with a high degree. As we have seen, we can always obtain the high quality entanglement characterized by inseparability $I_k \to 0$ as $G \to \infty$ by shaping the spectrum of LOs and LOi to a pair of decomposed modes and by increasing the gain coefficient G.

4.2. *The spectrum of the LO is not matched to any particular SVD mode*

In general, the LOs and LOi are not matched to any pair of the decomposed modes. The photocurrent out of HDs/HDi is contributed by all the temporal modes non-orthogonal to the spectrum of LOs/LOi (the mode-matching efficiency $|\xi_{ks}|^2 \neq 0/|\xi_{ki}|^2 \neq 0$, see Eq. (37)). Now let us analyze how the multi-mode nature of the twin beams affect the experimentally measured inseparability

$$I_{exp} = \langle \Delta \hat{X}_-^2 \rangle_{exp} + \langle \Delta \hat{Y}_+^2 \rangle_{exp}, \tag{40}$$

with

$$\langle \Delta \hat{X}_-^2 \rangle_{exp} = \frac{\langle \Delta(\hat{i}_s - \hat{i}_i)^2 \rangle}{q^2 |\alpha_{Ls}||\alpha_{Li}|} \Big\|_{\theta} \tag{41a}$$

$$\langle \Delta \hat{Y}_+^2 \rangle_{exp} = \frac{\langle \Delta(\hat{i}_s + \hat{i}_i)^2 \rangle}{q^2 |\alpha_{Ls}||\alpha_{Li}|} \Big\|_{\theta+\frac{\pi}{2}} \tag{41b}$$

denoting the measured variances of the correlation of quadrature-phase amplitudes of twin beams, where $\theta = \theta_{Ls} = \theta_{Li}$ refers to the phase of local oscillators. According to the expression of photocurrent in Eq. (37), we have

$$\langle \Delta \hat{X}_-^2 \rangle_{exp} = V_{Xs} + V_{Xi} - 2C_X \tag{42a}$$

$$\langle \Delta \hat{Y}_+^2 \rangle_{exp} = V_{Ys} + V_{Yi} + 2C_Y, \tag{42b}$$

with

$$V_{Xs} = V_{Ys} = \sum_{k=1}^{\infty} |\xi_{ks}|^2 [\cosh^2(r_k \times G) + \sinh^2(r_k \times G)]/2 \tag{43a}$$

$$V_{Xi} = V_{Yi} = \sum_{k=1}^{\infty} |\xi_{ki}|^2 [\cosh^2(r_k \times G) + \sinh^2(r_k \times G)]/2, \tag{43b}$$

and

$$C_X = \sum_{k=1}^{\infty} C_{Xk} = \sum_{k=1}^{\infty} |\xi_{ks}\xi_{ki}| \cosh(r_k \times G) \sinh(r_k \times G) \cos(\theta_{Ls} + \theta_{Li} + \theta_{ks} + \theta_{ki}), \tag{44a}$$

$$C_Y = \sum_{k=1}^{\infty} C_{Yk} = -\sum_{k=1}^{\infty} |\xi_{ks}\xi_{ki}| \cosh(r_k \times G) \sinh(r_k \times G) \cos(\theta_{Ls} + \theta_{Li} + \theta_{ks} + \theta_{ki}). \tag{44b}$$

#250441 Received 18 Sep 2015; accepted 27 Oct 2015; published 2 Nov 2015

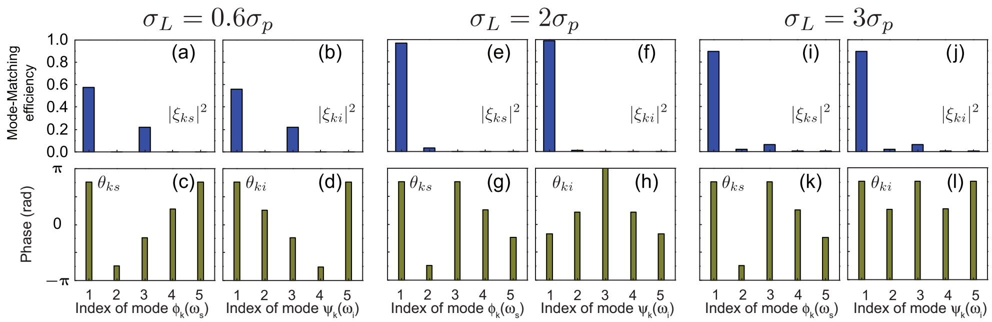

Fig. 3. Mode matching efficiency $|\xi_{ks}|^2$ ($|\xi_{ki}|^2$) and phase θ_{ks} (θ_{ki}) for the kth order decomposed signal (idler) mode $\phi_k(\omega_s)$ ($\psi_k(\omega_i)$) when the bandwidths of LOs and LOi are $\sigma_L = 0.6\sigma_p$ (plots (a)-(d)), $\sigma_L = 2\sigma_p$ (plots (e)-(h)), and $\sigma_L = 3\sigma_p$ (plots (i)-(l)), respectively. The parameters of the FOPA are the same as those in Fig.2

where $V_{Xs(i)}$ and $V_{Ys(i)}$ are the phase-independent noise variances for the signal (idler) field, and C_X and C_Y, which are sensitive to phase between the local oscillators and the signal and idler modes, respectively, are the correlation terms of the quadrature-phase amplitudes between the signal and the idler beams, respectively. Note that the minus sign in Eq. (44b) is originated from the $\pi/2$-phase difference between two quadrature components.

From Eqs. (40)-(44), one sees that the key to minimize the inseparability I_{exp} is to maximize the correlation terms in Eqs. (44a) and (44b) by adjusting the phase of the local oscillators θ_{Ls} and θ_{Li}. It is straightforward to maximize the individual terms C_{Xk} and C_{Yk} for a given mode index k in Eqs. (44a) and (44b), however, it is difficult to maximize the correlation term for all the terms with $|\xi_{ks}|^2 \neq 0/|\xi_{ki}|^2 \neq 0$, because the phase θ_{ks} and θ_{ki} may varies with the mode index k. This will generally result in a decrease in the measured degree of entanglement.

Having understood the measurement principle of entanglement, we are ready to study the parameters that will influence the degree of the measured quadrature amplitude entanglement generated by the FOPA analyzed in Sec. 2.3, which has a broad gain bandwidth in telecom band. Assuming the local oscillators LOs and LOi have the same bandwidth σ_L, but their central frequencies are the same as the corresponding signal and idler fields, the spectrum of LOs/LOi, which is Gaussian shaped and transform limited, can be expressed as:

$$A_{Ls(Li)}(\omega_{s(i)}) = \frac{1}{\sqrt{\pi^{1/2}\sigma_L}} \exp\{\frac{-(\omega_{s(i)} - \omega_{s0(i0)})^2}{2\sigma_L^2}\}. \tag{45}$$

We first analyze the mode matching of the homodyne detection systems. Using the twin beams with mode structure shown in Fig. 2 and substituting Eq. (45) into Eq. (36), we calculate the mode matching coefficient for each pair of the decomposed SVD modes. Figure 3 shows the calculated mode-matching efficiency and the phase for the kth order decomposed signal/idler mode $\phi_k(\omega_s)/\psi_k(\omega_i)$ when the bandwidths of LOs and LOi are $\sigma_L = 0.6\sigma_p$, $\sigma_L = 2\sigma_p$, and $\sigma_L = 3\sigma_p$, respectively. For each case, one sees that the phase $\theta_{ks(i)}$ of the signal (idler) mode varies with the index k, indicating that it is impossible to simultaneously obtain the maximized correlation terms C_{Xk} and C_{Yk} for each pair of decomposed modes. On the other hand, since only the modes with the non-zero mode matching efficiencies contribute to the measurement of HDs and HDi, Fig. 3 shows that the main contribution is from the modes with index number $k < 5$. Moreover, for the mode with a fixed index number, the mode matching coefficient varies with the bandwidth σ_L. For the case of $\sigma_L = 0.6\sigma_p$ (Figs. 3(a)-(d)), the sum of mode-matching efficiency for the first- and third-order modes are about 90%, and the mode matching efficiency

#250441 Received 18 Sep 2015; accepted 27 Oct 2015; published 2 Nov 2015

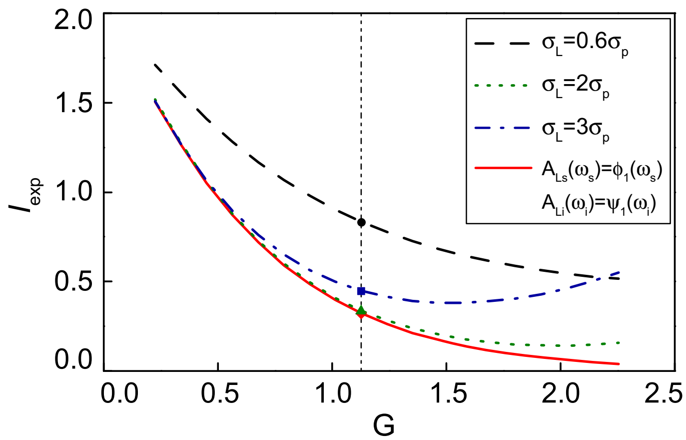

Fig. 4. Measured inseparability of twin beams, I_{exp}, as a function of gain coefficient G when the bandwidths of LOs and LOi are $\sigma_L = 0.6\sigma_p$, $\sigma_L = 2\sigma_p$ and $\sigma_L = 3\sigma_p$, respectively. As a comparison, I_{exp}=I_1 for the LOs and LOi with the spectra the same as the fundamental modes $\phi_1(\omega_s)$ and $\psi_1(\omega_i)$ is also plotted. The results obtained for the JSF in Fig. 2 are marked by cross points between the data and dashed line.

for the other modes are too small to be obviously observed; for the case of $\sigma_L = 3\sigma_p$ (Figs. 3(i)-(l)), the mode matching efficiency for the first order is about 90%. While for the case of $\sigma_L = 2\sigma_p$ (Figs. 3(e)-(h)), the mode matching is obviously better than the other two cases because the mode-matching efficiency for the first order mode is very close to 1.

We then study the dependence of the measured degree of entanglement upon the mode matching of HDs and HDi by numerically calculating the inseparability I_{exp} in different conditions. Figure 4 shows the calculated I_{exp} as a function of the gain coefficient G when the bandwidths of LOs and LOi are $\sigma_L = 0.6\sigma_p$, $\sigma_L = 2\sigma_p$, and $\sigma_L = 3\sigma_p$, respectively. In the calculation, for each gain coefficient, we deduce the corresponding mode structure and mode matching for different spectrum of LOs and LOi, which is similar to the procedure of obtaining the plots in Figs. 2 and 3. The results corresponding to the JSF in Fig. 2 are marked by cross points between the data and the dashed line. Additionally, as a comparison, the inseparability I_1 for LOs and LOi with the spectra the same as the corresponding fundamental modes $\phi_1(\omega_s)$ and $\psi_1(\omega_i)$ is also plotted in Fig. 4 as a function of G. Obviously, for a fixed gain coefficient G, the value of I_1 is always smaller than that of I_{exp}.

In Fig. 4, when the spectra of LOs and LOi are not matched to the fundamental modes, one sees that for a fixed value of G, the lowest and highest I_{exp} respectively correspond to the case of $\sigma_L = 2\sigma_p$ and $\sigma_L = 0.6\sigma_p$. If we compare the mode matching efficiency in Fig. 3, it is straightforward to see that the measured degree of entanglement increase with the mode matching efficiency between the local oscillators and the fundamental modes, $|\xi_{1s}|^2$ and $|\xi_{1i}|^2$, and the departure between I_{exp} and I_1 will increase when the spectra of LOs and LOi are more evenly distributed among the decomposed othogonal modes.

From Fig. 4, one also sees that different from I_1, which always decreases with the increase of G, the measured I_{exp} may increase with G when G is larger than a certain value. For the case of $\sigma_L = 3\sigma_p$, it is obvious that I_{exp} start to increase with G for $G > 1.4$. For the case of $\sigma_L = 2\sigma_p$, this kind variation trend is also observable: I_{exp} increases with G for $G > 1.9$. We think the reason is because the the correlation term C_{Xk}/C_{Yk} (see Eqs. (44a) and (44b)) for different k can not simultaneously achieve the maximum for the LOs/LOi with a given phase. Although the mode matching efficiency of the first order mode is the highest (see Fig. 3), the

#250441 Received 18 Sep 2015; accepted 27 Oct 2015; published 2 Nov 2015

noise variance of I_{exp} contributed by the signal and idler beams in higher order SVD modes may exponentially increase with G, which will results in the unusual trend of I_{exp}. Moreover, it is worth noting that the influence of mode mismatching effect on measured entanglement is not equivalent to an effective detection loss because the noise contributed by higher order modes with $|\xi_{ks}|^2 \neq 0/|\xi_{ki}|^2 \neq 0$ will become significant, particularly in the high gain regime of FOPA.

5. Conclusion

In summary, we theoretically analyzed the temporal mode structure and the degree of measured CV entanglement of the twin beams generated from a pulse-pumped FOPA by applying the SVD to the JSF. We are able to successfully decouple different temporal modes and derive the input-output relation for each temporal mode. The results indicate that the temporal mode structures are highly sensitive to the dispersion of the nonlinear fiber and the gain coefficient of FOPA. While for the measurement of CV entanglement, when the temporal modes of LOs and LOi are the same as one pair of decomposed modes, $\phi_k(\omega_s)$ and $\psi_k(\omega_i)$, the measurement result of the homodyne detection systems is only contributed by the signal and idler fields in the modes $\phi_k(\omega_s)$ and $\psi_k(\omega_i)$, which is similar to case of pulsed pumped parametric amplifier having a factorizable JSF; when the modes of LOs and LOi can not match any pair of the decomposed modes, the measurement result of the homodyne detection systems is contributed by all the modes non-orthogonal to the spectra of local oscillators, leading to a poor value of the inseparability. Therefore, in order to obtain the high degree CV entanglement, making the JSF factorable is not necessary, but matching the spectra of local oscillators to one pair of decomposed modes is crucial. Moreover, for the FOPA with broad gain bandwidth of FWM in telecome band, we numerically studied the temporal mode functions of the twin beams, and calculated its corresponding degree of CV entanglement when the spectra of LOs and LOi of HD systems are varied. The results demonstrate the detailed temporal mode structure of this kind of FOPA as well as the strategy for optimizing the spectra of the local oscillators in the detection process. Hence, our study is useful for developing a high-quality source of pulsed CV entanglement by using the FOPA.

Our investigation indicates that the determination of the JSF, including the absolute value ($|F(\omega_s', \omega_i')|$) and the phase term $\arctan(\frac{Re\{F(\Omega_s,\Omega_i)\}}{Im\{F(\Omega_s,\Omega_i)\}})$, is utmost important for the mode analysis of a pulse-pumped parametric process. So far, the measurements of the absolute value of JSF have been demonstrated [29–32]. If there is a practical scheme to realize the measurement of the phase term of JSF, which has not been reported yet, it will be straightforward to realize the required mode matching by shaping the spectra of LOs and LOi [33].

Acknowledgment

This work was supported in part by the National NSF of China (No. 11527808, No. 11304222), the State Key Development Program for Basic Research of China (No. 2014CB340103), the Specialized Research Fund for the Doctoral Program of Higher Education of China (No. 20120032110055), PCSIRT and 111 Project B07014.

#250441 Received 18 Sep 2015; accepted 27 Oct 2015; published 2 Nov 2015